ELSEVIER

Tectonophysics 269 (1997) 113–129

TECTONOPHYSICS

New paleomagnetic data from the Mongol–Okhotsk collision zone, Chita region, south-central Russia: implications for Paleozoic paleogeography of the Mongol–Okhotsk ocean

Xi Xu [a], William Harbert [a,*], Sergei Dril [b], Vadim Kravchinksy [c]

[a] *Department of Geology and Planetary Science, University of Pittsburgh, Pittsburgh, PA 15260-3332, USA*
[b] *Institute of Geochemistry, Academy of Sciences of Russia, Irkutsk, Russia*
[c] *Research Branch, Ministry of Geology, Irkutsk, Russia*

Received 10 July 1995; accepted 24 June 1996

Abstract

We present a reconnaissance paleomagnetic study of rocks from several formations of the Chita region of south-central Russia (representative location $\lambda = 51°N$, $\phi = 116°E$), within the Mongol–Okhotsk collision zone. Sections of siltstone and fine-grained sandstone, dated using fossils as Bashkirian to Moscovian epochs (USSR Carboniferous system, Middle Carboniferous), Early Permian, Late Permian and Triassic in age were sampled. The resulting collection from five stratigraphic sections is a total of 319 oriented samples from 51 sites. Generally, 5 to 10 samples per site were collected. Sample orientation was determined using both magnetic and sun-shadow azimuths. All paleomagnetic measurements were completed in the Paleomagnetic Laboratory at the University of Pittsburgh using a 3-component 2G Superconducting Rock Magnetometer (SRM) in a magnetically shielded room. Thermal demagnetization was completed using between 12 to 20 heating steps up to temperatures of 685°C. Principal component analysis of the demagnetization data was successful in isolating two characteristic remanent magnetizations. The lower unblocking temperature component, component A, fails the fold test, is always of downward directed magnetic inclination, and may record the present-day Earth's (PDF) magnetic field [PDF $I = 69.4°$, $D = 351.8°$; component A, $I_g = 65.1°$, $D_g = 356.5°$, $\alpha_{95} = 6.2°$, N (sites) $= 50$]. The higher unblocking temperature magnetic component (B), was observed in the Triassic (B_T, $N = 3$), Late Permian (B_{LP}, $N = 14$), Early Permian (B_{EP}, $N = 5$) and Bashkirian to Moscovian epochs of the Late Carboniferous (B_{MC}, $N = 8$) sections. The B component differs significantly from component A, and is recorded by sites of both downward and upward directed magnetic inclinations in the Late Permian and Bashkirian to Moscovian epoch sections. Component B_{MC} and B_{LP} may represent primary remanent magnetizations. The Bashkirian to Moscovian epochs of the Late Carboniferous mean paleolatitude is $\lambda_{MC} = 19.9° \pm 14.8°$ and the Late Permian mean paleolatitude is $\lambda_{LP} = 19.6° \pm 14.5°$. Both are similar to that expected from reference paleomagnetic poles from the North China block, but significantly different from paleolatitudes calculated using reference poles from the Siberian or European plates. We interpret the results of this study to suggest that the sampled sections were located near, or associated with, the North China Block during their deposition.

Keywords: paleomagnetism; Paleozoic; paleogeography; plate tectonics; Mongol–Okhotsk collision zone

* Corresponding author. Fax: +1.412-624-3914; e-mail: harbert + @pitt.edu

PII S0040-1951(96)00140-0

1. Introduction

The Mongol–Okhotsk belt is a broad collision zone which stretches southwest–northeast across the entire central portion of eastern Asia. Bordering this complex collision zone, to the southeast is the North China Block (Sino–Korea Block), to the southwest the Tarim block and Jungar block, and to the north the Siberian and Eurasian plates. The Mongol–Okhotsk formed during the closure of the Mongol–Okhotsk ocean (occasionally referred to as the Paleo-Tethys or Paleo-Okhotsk ocean) and collision and suturing of blocks and microplates to the Siberian and Eurasian plates. Previous summaries of the research conducted in this region include Zonenshain et al. (1990) (which is mainly based on the geologic and paleomagnetic research of Russian scientists) and Enkin et al. (1992) (which summarized the paleomagnetic data including many recent Chinese paleomagnetic results).

Zonenshain et al. (1990) summarized the geologic research results of Russian geologists who felt that the Mongol–Okhotsk belt is composed of a series of small blocks or tectonostratigraphic terranes, including the North Mongolia, West Trans-Baikal (to the north), Khingan–Bureya, Argun and Central Mongolian massifs (to the south). Convergence-related complexes such as subduction-related volcanic complexes are found south of the Mongol–Okhotsk belt leading Zonenshain et al. (1990) to suggest that blocks within the Chita region of the Mongol–Okhotsk belt accreted with the Siberian plate during the Paleozoic.

Low Paleozoic paleolatitudes have been shown using paleomagnetic data for the Tarim (Li et al., 1988a,b; McFadden et al., 1988; Sharps et al., 1989; Li, 1990; Li et al., 1990; Nie et al., 1993), Jungar (Li et al., 1991), Qiliangshan (Li and Zhang, 1986; Li et al., 1989), North China Block (Enkin et al., 1992), Mongolian terranes (Pruner, 1987, 1992; Zhao and Coe, 1987; Zhao et al., 1990), and South China Block (Lin et al., 1985; Lin and Fuller, 1986). Interpretation of paleoclimatic data also suggests low paleolatitudes for these terranes (Nie et al., 1990; Nie, 1991).

Enkin et al. (1992) presented plate tectonic reconstructions which showed tectonostratigraphic terranes of the Mongol–Okhotsk belt located far south of the Siberia plate before the Middle Paleozoic. In the model of Enkin et al. (1992), these blocks, including blocks located in the Chita region, were accreted to the Eurasian plate during the Cretaceous.

By sampling units of the Bashkirian to Moscovian epochs, Early and Late Permian, and Triassic age we hoped to determine a series of paleolatitudes to constrain plate tectonic models describing the formation of this collision zone. Sections were sampled at two regions in southern Siberia. A Carboniferous section, an Early Permian section and a Triassic section were collected near the Ingoda river. Two exposures of a Late Permian section were sampled near the village of Biliktui.

2. Geology of the Chita region, Russian Republic

The Mongol–Okhotsk belt has been interpreted to represent a typical intercontinental foldbelt resulting from the collision of North China, Tarim, Jungar and smaller Mongol–Okhotsk blocks (Fig. 1) (Zonenshain et al., 1990) with the Siberian plate. The relative position of these blocks during the Paleozoic and their accretion and collision ages have been constrained using paleomagnetism and paleontology. Using reference paleomagnetic data from the stable Siberian plate, expected Devonian paleolatitudes for our sampling region are between 55°N–60°N (Khramov, 1982; Pechersky and Didenko, 1995); however, Coral-reef limestones found in a Devonian sequence have been interpreted to show that at least some of the Mongol–Okhotsk belt blocks were located in a low latitude region (Zonenshain et al., 1990).

Zonenshain et al. (1990) cite geologic evidence which suggests that the Mongol–Okhotsk blocks first collided with the Siberian plate during the Middle Carboniferous to Permian. Within the Mongol–Okhotsk belt, observations cited to support this interpretation include Jurassic aged metamorphism and formation of granite–gneissic domes and Triassic aged intrusion of gabbro–tonalites. Zonenshain et al. (1990) interpret these data to suggest a Mongol–Okhotsk–Siberian plate affinity and subduction of oceanic crust along a northward-dipping subduction zone, beneath the Mongol–Okhotsk belt during the Mesozoic. In addition, subduction beneath portions

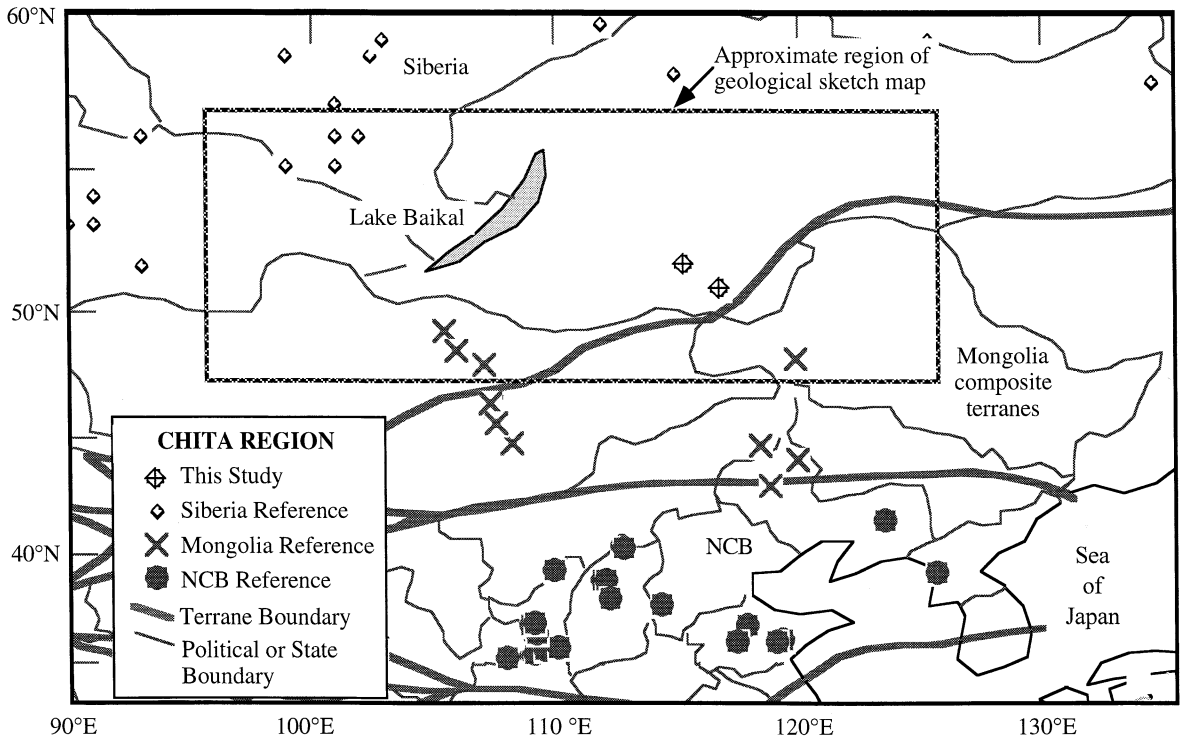

Fig. 1. Reference map of the present-day geography of the Chita region in southern Russia. Paleomagnetic reference sites from the Mongolia composite terranes, North China Block and the Siberian plate are shown. These data were extracted from Version 2.3 of the Global Paleomagnetic Database (McElhinny and Lock, 1990). The location of the two new sampling localities and the approximate outline of the geological map given in Fig. 2 are also shown.

of the southern edge of the Siberian plate is suggested by Jurassic nearshore and marine forearc in the Uda region, Middle Jurassic to Early Cretaceous age plutonism (K/Ar ages 118–176 Ma) in the Uda arc, and Middle Jurassic to Early Cretaceous age metamorphism along the west Dzhagdy zone. Zonenshain et al. (1990) suggested that Mongol–Ohkotsk blocks welded completely with the Siberia plate by Middle Jurassic, closing the ''Paleo-Okhotsk'' (Mongol–Okhotsk) ocean. In this model, the North China block collided and welded with the composite Mongol–Okhotsk blocks–Siberia plate no later than 120–140 Ma.

In contrast, Enkin et al. (1992) suggest that the Mongolia–Okhotsk blocks collided with the North China block during the Late Permian. In this model, the Tarim and Jungar blocks were sutured with the Eurasia plate earlier than the composite Mongolia–North China block. Most models suggest final consolidation of the North China Block and terranes within the Mongolian region during the Late Permian (Nie et al., 1990; Zhao et al., 1990; Yin and Nie, 1993). The initial collision between the South China Block and North China Block appears to have occurred during the Triassic, with final amalgamation of the South China Block and North China Block occurring during the middle Jurassic (Nie et al., 1990).

Enkin et al. (1992) have suggested that the composite ''Chinese Block'', consisting of the North and South China blocks, Korea and Mongolia terranes collided with the Eurasia–Siberian plate at about the position of the current west end of the Mongol–Okhotsk belt. The open ocean between the composite Chinese block and Siberia was approximately 1000 km wide in Upper Jurassic. Estimates of the time of closure of the Mongol–Okhotsk ocean, or accretion of the Chinese composite terrane to the Siberian

plate range from Early Cretaceous (Enkin et al., 1992) or 120–140 Ma (Zonenshain et al., 1990) to Late Cretaceous (Zheng et al., 1991). A key distinction between these models is whether the Mongol–Okhotsk blocks sampled paleomagnetically in this study were associated with the southern Siberia plate margin (Zonenshain et al., 1990) or the North China Block and other Chinese blocks (Enkin et al., 1992) before accretion of the North China Block to Siberia.

3. Sample collection and demagnetization

The sampling areas are located in the Chita region, south-central Russia, near the eastern intersection of the political border zones of Russia, Mongolia and China (Fig. 2). The Ingoda and Biliktui locations were chosen because of their relatively good exposure of Carboniferous to Triassic strata. A total of 319 samples from 51 sites were collected; samples were collected from a Bashkirian to Moscovian epoch age section (16 sites), Early Permian section (6 sites), Late Permian section (26 sites from 2 adjacent sections) and a Triassic section (3 sites).

Five to ten samples were collected from each site using a gasoline powered drill. Before the samples were removed from the rock bed the orientation was determined using both magnetic compass and sun-shadow azimuth. The sun compass was used to determine the difference between geographic and magnetic north at each locality. The average of these sun compass shadow angles closely matched (within

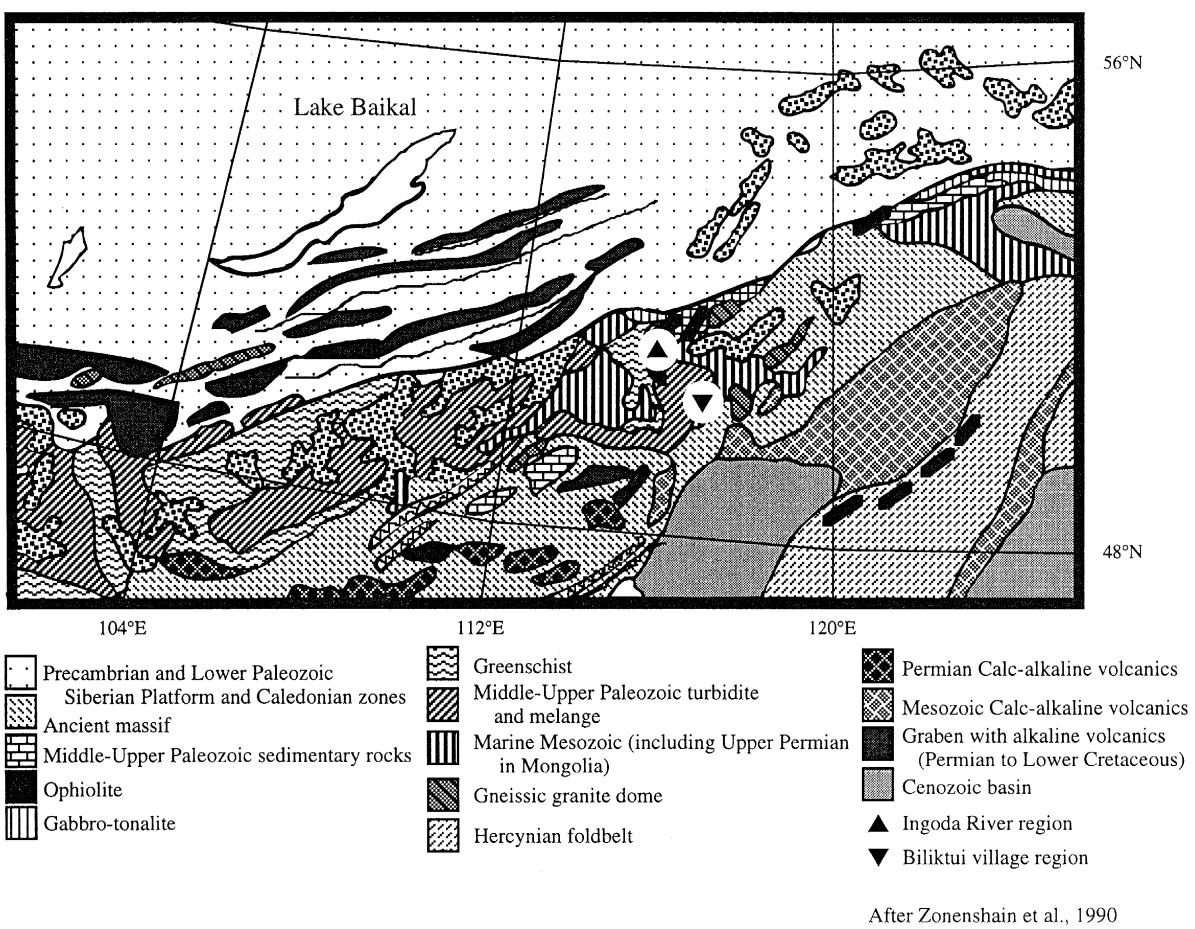

Fig. 2. This figure, redrafted from Zonenshain et al. (1990), shows the simplified regional geology of the sampling region.

0.2°) expected differences between true and magnetic north calculated from spherical harmonic models of the Earth's magnetic field for the field sites. The bed attitudes were recorded as dip vectors, and azimuths and plunges were recorded using both Russian and American compasses and communicated in both English and Russian. Field notes were also recorded in both languages for maximum clarity. Field work took approximately 4 weeks.

The first sampled section is located near the Ingoda river (Fig. 3: coordinates: 51.53°N, 115.39°E), where the Carboniferous Tutchaltuiskaia and Charashibirskaia Suites are located. Ages are assigned to these suites using the U.S.S.R. Carboniferous system which divides the Carboniferous period into three sub-periods, Early, Middle and Late Carboniferous (Harland et al., 1982). The Middle Carboniferous in this system corresponds to the Bashkirian and Moscovian epochs (which are within the Late Carboniferous of the IUGS Carboniferous Period representation of the geologic time scale). The Tutchaltuiskaia Suite is composed of Early to Middle Carboniferous argillite with layers of sandstone and conglomerate. Our sampling of the Tutchaltuiskaia Suite took place within the Middle Carboniferous portion. The Charashibirskaia Suite is composed of the same sedimentary lithologies of Middle Carboniferous age. An Early Permian sequence of argillite and fine-grained sandstones and Triassic basalt flows were also sampled in this region.

The other sampled region is near the small village of Biliktui (Fig. 4: coordinates: 50.65°N, 116.88°E).

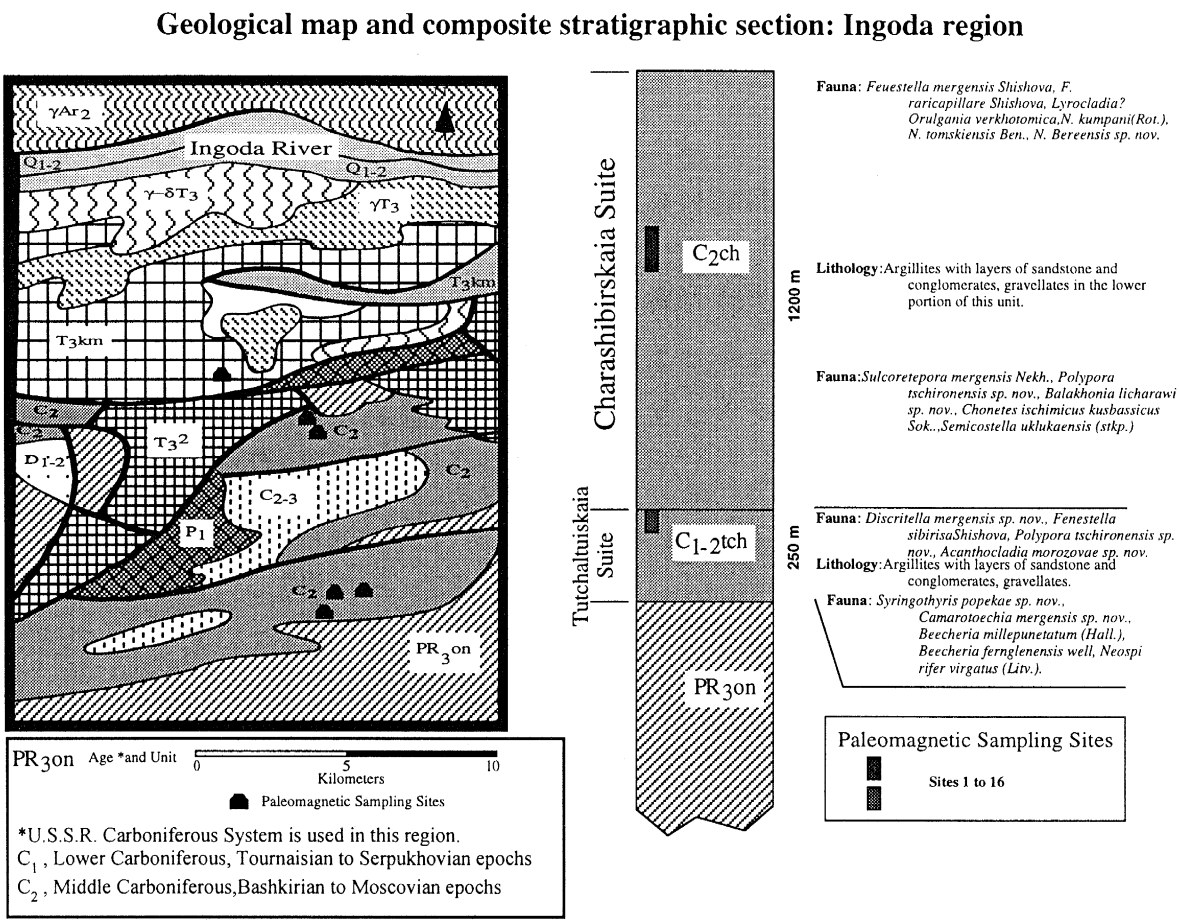

Fig. 3. Geologic sketch map and stratigraphic column for the Ingoda River locality.

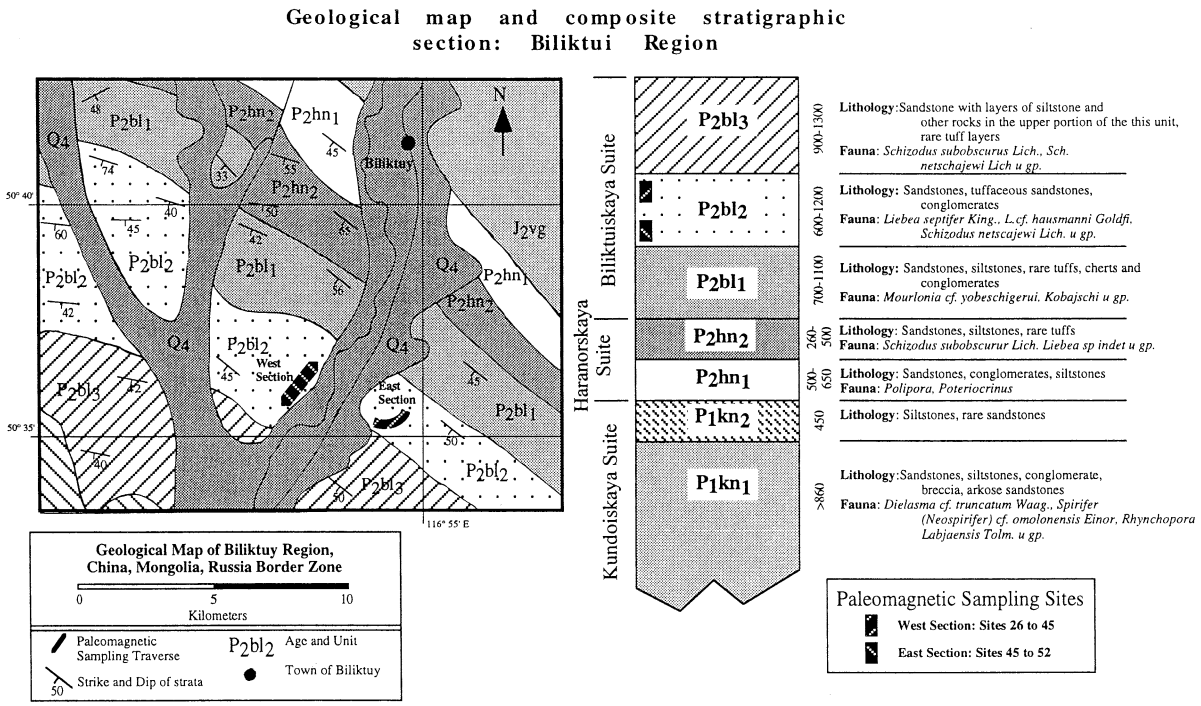

Fig. 4. Geologic sketch map and stratigraphic column for the Biliktui village locality.

Here the Biliktuiskaya Suite is composed of three differentiated Late Permian sedimentary units. The sampled P2Bl2 section is the middle member of this suite and has a stratigraphic exposure of about 600–1200 m. It consists of fine- to medium-grained sandstones, tuffaceous sandstones, and conglomerates. Samples were collected from the fine-grained sandstones along both sides of the Bereya river valley. Bedding dip vectors were directed generally to the southwest with dips of between 40°–60°.

After collection these samples were transported to the Paleomagnetism Laboratory at the University of Pittsburgh. Core samples were then cut into core specimens that were 25.4 mm in diameter and height. The laboratory treatment of these rocks included stepwise thermal demagnetization and remanent magnetization measurements using the 2G SRM. The samples were stepwise thermally demagnetized using an ASC TD-48 Thermal Specimen Demagnetizer. Principal component analysis was applied to the resultant magnetization vectors in geographic coordinates to determine best fitting linear segments to the demagnetization data.

4. Paleomagnetic analysis

After stepwise thermal demagnetization, principal component analysis was applied to the demagnetization data. Originally, five magnetic components were thought to have been identified. However after fitting these components to all samples and then calculating both Bingham and Fisher mean directions for each component it was determined that two sets of two magnetic components did not significantly differ, these were combined into a lower temperature (A), and higher temperature (B), magnetic component. An intermediate unblocking temperature magnetic component, highly scattered, even within a single paleomagnetic site, appeared to be random between samples and sites and was deleted from further analysis. The magnetic A component was generally observed in the thermal demagnetization step interval of between room temperature and about 300°C (Fig. 5).

The A magnetic component is always of downward directed magnetic inclination and showed best clustering in geographic coordinates (Tables 1 and

Table 1
Statistical results of component A and component B lines

Site	Age	Component A				Component B				Bedding correction	
		N	I_g	D_g	k	N	I_g	D_g	k	Strike	Dip
SIB01	C_2^*	4	29.6	336.3	5.1	2	−29.6	288.3	3.3	253.0	38.0 N
SIB02	C_2^*	5	53.5	25.2	2.8	2	18.0	126.4	3.8	257.0	38.0 N
SIB03	C_2^*	5	57.0	346.3	16.1	3	−12.3	124.3	4.8	251.0	38.5 N
SIB04	C_2^*	5	76.4	13.6	2.5	2	24.3	132.7	7.8	250.0	40.0 N
SIB05	C_2^*	5	71.1	4.9	3.9	1	42.2	99.7	–	252.0	38.0 N
SIB06	C_2^*	4	58.5	60.2	15.0	1	63.9	56.4	–	262.0	35.0 N
SIB07	C_2^*	6	59.6	45.1	4.6	2	7.7	100.4	4.2	242.0	35.0 N
SIB08	C_2^*	7	29.1	310.1	9.2	4	2.3	284.6	14.2	232.0	35.0 N
SIB09	C_2^*	6	81.1	324.0	12.2	–	–	–	–	232.0	35.0 N
SIB10	C_2^*	4	58.4	355.1	7.2	1	−31.6	114.0	–	232.0	40.0 N
SIB11	C_2^*	6	62.6	359.2	13.4	2	39.9	129.7	6.0	336.0	32.0 N
SIB12	C_2^*	7	52.3	354.7	8.0	1	32.1	35.8	–	336.0	25.0 N
SIB13	C_2^*	7	73.1	308.9	10.9	–	–	–	–	326.0	31.0 N
SIB14	C_2^*	7	69.2	29.2	5.8	3	55.7	65.6	9.7	328.0	29.0 N
SIB15	C_2^*	6	62.1	354.7	19.6	–	–	–	–	309.0	29.0 N
SIB16	C_2^*	6	65.9	39.5	9.4	1	41.8	28.3	–	309.0	29.0 N
SIB17	P_1	5	81.2	25.3	7.2	2	55.7	181.8	2.4	332.0	70.0 N
SIB18	P_1	7	75.5	315.2	5.9	5	79.1	213.1	5.8	332.0	70.0 N
SIB19	P_1	7	34.3	23.2	2.8	1	13.7	146.1	–	327.0	67.0 N
SIB20	P_1	8	72.3	333.3	18.1	3	52.1	249.6	12.0	327.0	67.0 N
SIB21	P_1	5	55.4	13.4	13.6	3	40.2	234.2	9.4	336.0	71.0 N
SIB22	P_1	9	62.6	237.2	8.9	4	56.0	263.3	29.0	325.0	69.0 N
SIB23	Tr	6	82.2	246.7	80.3	6	21.1	113.8	63.2	262.0	31.0 N
SIB24	Tr	4	72.9	80.6	31.6	6	26.9	102.0	15.3	262.0	31.0 N
SIB25	Tr	4	41.4	345.5	33.1	5	48.3	25.0	61.6	262.0	31.0 N
SIB26	P_2	6	76.6	324.0	4.7	3	43.0	102.5	3.3	106.5	40.0 S
SIB27	P_2	5	77.6	14.5	8.6	2	38.1	108.9	12.4	96.5	40.0 S
SIB28	P_2	4	57.0	355.9	3.6	2	−17.8	215.0	13.5	91.5	45.0 S
SIB29	P_2	4	39.4	353.7	10.9	2	31.4	53.9	4.0	89.0	45.0 S
SIB30	P_2	4	60.0	335.3	16.4	5	−18.7	286.8	3.7	73.5	42.0 S
SIB31	P_2	6	80.3	290.7	3.7	3	−43.5	212.5	2.9	84.5	47.0 S
SIB32	P_2	7	54.4	5.0	7.3	1	−28.4	292.2	–	96.5	57.5 S
SIB33	P_2	5	71.8	337.3	23.4	4	−22.9	247.8	3.9	102.5	51.0 S
SIB34	P_2	5	67.6	348.6	38.5	2	16.5	102.7	3.9	96.5	53.5 S
SIB35	P_2	5	49.4	4.7	12.8	3	23.5	54.2	5.8	98.5	55.0 S
SIB36	P_2	6	34.5	327.1	3.6	5	−38.2	308.95	3.7	121.5	40.0 S
SIB37	P_2	6	76.6	354.9	7.5	3	−9.3	255.2	5.4	121.5	40.0 S
SIB39	P_2	9	72.7	52.2	4.9	3	−47.0	246.2	27.8	121.5	5.0 S
SIB40	P_2	5	57.6	347.5	8.7	3	41.2	74.7	6.5	141.5	5.0 S
SIB41	P_2	6	64.8	0.5	5.4	2	0.4	51.4	524.2	131.5	15.0 S
SIB42	P_2	5	75.6	350.0	13.8	2	−23.7	251.5	2.5	111.5	50.0 S
SIB43	P_2	5	75.0	248.4	8.6	4	−47.0	246.0	5.5	96.5	53.0 S
SIB44	P_2	4	56.8	323.1	159.9	3	−41.0	278.8	6.7	91.5	45.0 S
SIB45	P_2	6	47.5	347.1	10.2	2	−51.8	287.8	4.3	106.5	45.0 S
SIB46	P_2	6	55.9	355.6	7.8	3	21.9	242.7	7.5	128.5	60.0 S
SIB47	P_2	5	61.4	329.3	7.6	4	−13.0	44.5	16.6	106.5	40.0 S
SIB48	P_2	5	61.7	356.6	3.6	2	−13.2	233.7	8.3	116.5	55.0 S
SIB49	P_2	–	–	–	–	4	9.5	106.0	6.5	106.5	50.0 S
SIB50	P_2	5	67.9	80.4	135.7	4	46.6	66.2	4.3	121.5	40.0 S
SIB51	P_2	5	12.9	86.4	57.4	5	−3.7	86.9	53.9	116.5	37.5 S
SIB52	P_2	5	4.9	332.9	12.3	4	−20.3	287.5	3.3	106.5	35.0 S

Ages: C_2^*, Bashkirian to Moscovian epochs of the Late Carboniferous; Tr, Triassic; P_1, Early Permian; P_2, Late Permian.

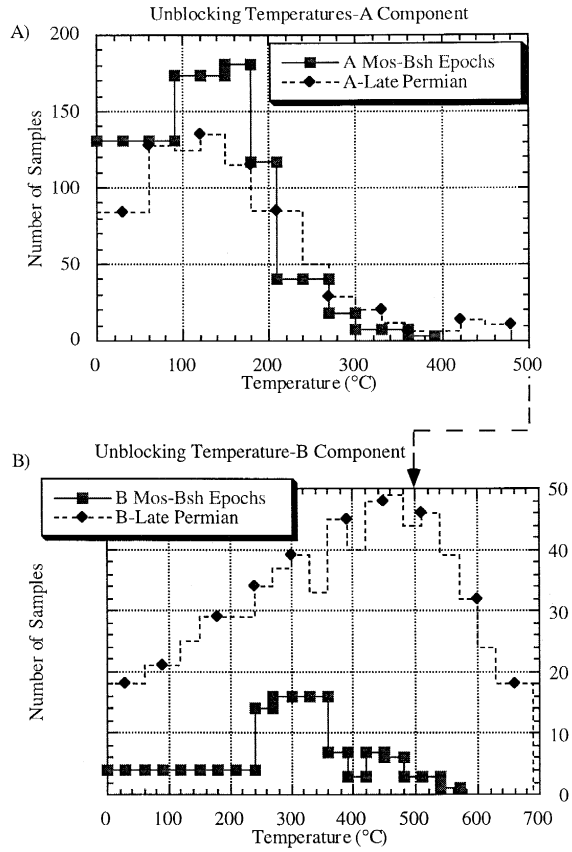

Fig. 5. Temperature unblocking spectra for A and B magnetic components from the Bashkirian and Moscovian epochs of the Late Carboniferous and Late Permian samples.

2). The fold test was applied to the site-mean magnetic directions for each section. Because of the similarity of the A magnetic component in all sampled sections, all sites which displayed an A component were combined and a regional fold test was applied to these data. Unfolding shows that the precision parameter k decreases with increasing tilt correction, suggesting that the A component magnetization is post-folding. The k-value (Fisher estimate of kappa) decreases from 11.6 in geographic coordinates to 3.2 in stratigraphic coordinates (k_0-value/k_{100}-value = 3.6, $n = 50$). The mean A component for all sites is $I_g = 65.1°$, $D_g = 356.5°$, k-value = 11.6, $\alpha_{95} = 6.2°$, n(sites) = 50. This direction closely matched the present-day Earth's (PDF) magnetic field expected for this site. For a representative location (51°N, 116°E) the expected PDF direction is $I = 69°$, $D = 352°$. The A component paleomagnetic magnetic pole, calculated from all sites in geographic coordinates, is $\lambda = 85.5°$N, $\phi = 328.0°$ $dm = 10.0°$, and $dp = 8.1°$, n(sites) = 50. Converting the paleomagnetic sites to paleomagnetic poles and then calculating a fisher average of these poles yields a mean A component paleomagnetic pole of $\lambda = 87.7°$N, $\phi = 6.8°$, $A_{95} = 8.0°$.

The higher unblocking temperature B magnetic component is more complex. The section of Bashkirian to Moscovian age in the Ingoda region consisted of 16 sites (SIB01-16). A total of 13 sites record a B component. We calculated Fisher statistics during partial unfolding using sites with n (samples) ≥ 2. The highest k-value is reached at 88% unfolding, although the change in the k-value between 88% and 100% unfolding is not significant (k_{100}-value = 14.5, k_{88}-value = 14.6, k_0-value = 8.3, k-value ratio k_{100}-value/k_0-value = 1.74, n(sites) = 8; Table 3). Two of these sites record a westerly directed characteristic magnetization. The paleolatitude $\pm A_{95}$ is $19.9° \pm 14.8°$, calculated from the

Table 2
Statistical analysis of the A component

Sites	Age	n	I_g	D_g	k-value	α_{95}	I_s	D_s	k-value	α_{95}
SIB01-16	C_2^*	16	63.9	359.7	14.8	9.9	34.3	1.7	7.9	14.0
SIB17-22	P_1	6	72.2	353.9	9.0	23.7	13.1	43.1	9.4	23.1
SIB23-25	Tr	3	74.5	358.2	6.8	51.5	43.6	354.3	6.8	51.5
SIB26-52	P_2	25	62.9	354.8	10.7	9.3	72.6	224.1	8.1	11.0
SIB01-52	–	50	65.1	356.5	11.6	6.2	68.3	356.4	3.2	13.6

Site name, age, number of sites (n), locality, coordinates of geographic and stratigraphic inclination (I_g, I_s), declination (D_g, D_s), Fisher estimate of kappa, (k-value), and cone of 95% confidence (α_{95}). The Bashkirian and Moscovian epochs of the Late carboniferous (C_2^*), Early Permian (P_1) and Triassic (Tr) sites are located in the Ingoda river region (51.53°N, 115.39°E) the Late Permian (P_2) sites are located in the Biliktui village region (50.65°N, 116.88°E) of southern Siberia.

Fisher average of paleomagnetic poles for sites with n (samples) ≥ 2.

Because of the very limited time available to sample these units and the long trek required to reach them, the Triassic section from the Ingoda region consists of three sites and 17 samples (SIB23-25) (Fig. 6). These units were the only igneous flows sampled, and displayed a stable and linear demagne-

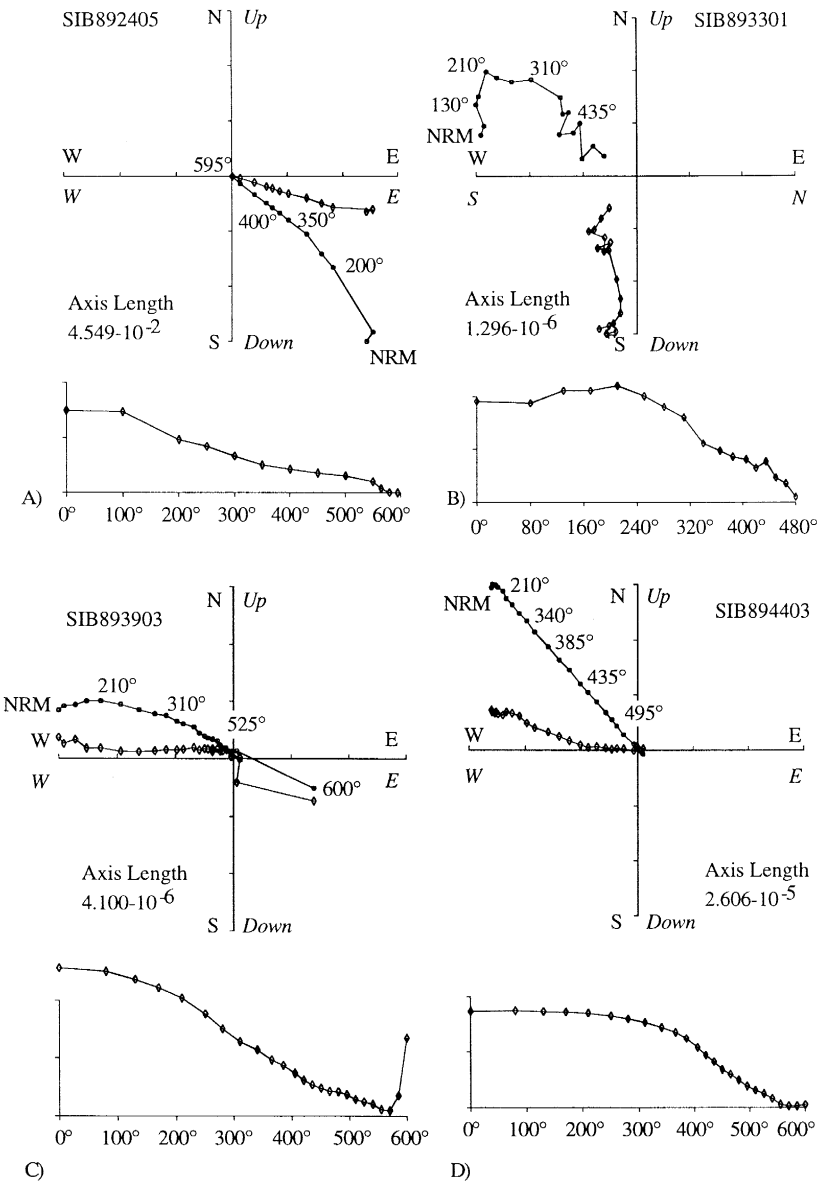

Fig. 6. Representative orthogonal vector plots in geographic (in-situ) coordinates and thermal demagnetization intensity decay diagrams. Symbols used, circles = projection of demagnetization data into a vertically oriented plane, diamonds = projection of demagnetization data into a horizontally oriented plane. Samples plotted are (A) SIB892405–Triassic igneous flow, (B) SIB893301–Late Permian Biliktuiskaya Suite sedimentary unit, (C) SIB893903–Late Permian Biliktuiskaya Suite sedimentary unit, and D) SIB894403–Late Permian Biliktuiskaya Suite sedimentary unit.

tization. The B component is observed in this section. Unfortunately, while a reconnaissance mean can be calculated, no meaningful statistical error estimates can be determined.

The Early Permian section from the Ingoda region consists of 6 sites (SIB17-22). We calculated Fisher statistics during partial unfolding using sites with $n \geq 2$. From a total of 5 sites, the B_{EP} component directions from this section show no significant difference in grouping between geographic and stratigraphic coordinates ($k_{100}/k_0 = 0.79$, $n = 5$; Fig. 7). All B component directions are of downward directed magnetic inclination. In geographic coordinates the B_{EP} component direction is $I_g = 59.8°$, $D_g = 232.3°$, k_g-value = 13.8. The stratigraphic B_{EP} component direction is $I_s = 50.4°$, $D_s = 66.8°$, k_s-value = 10.9 (Fig. 8). The paleolatitude and A_{95} calculated from the Fisher average of site paleomagnetic poles is $24.4° \pm 26.3°$.

A higher unblocking temperature B component

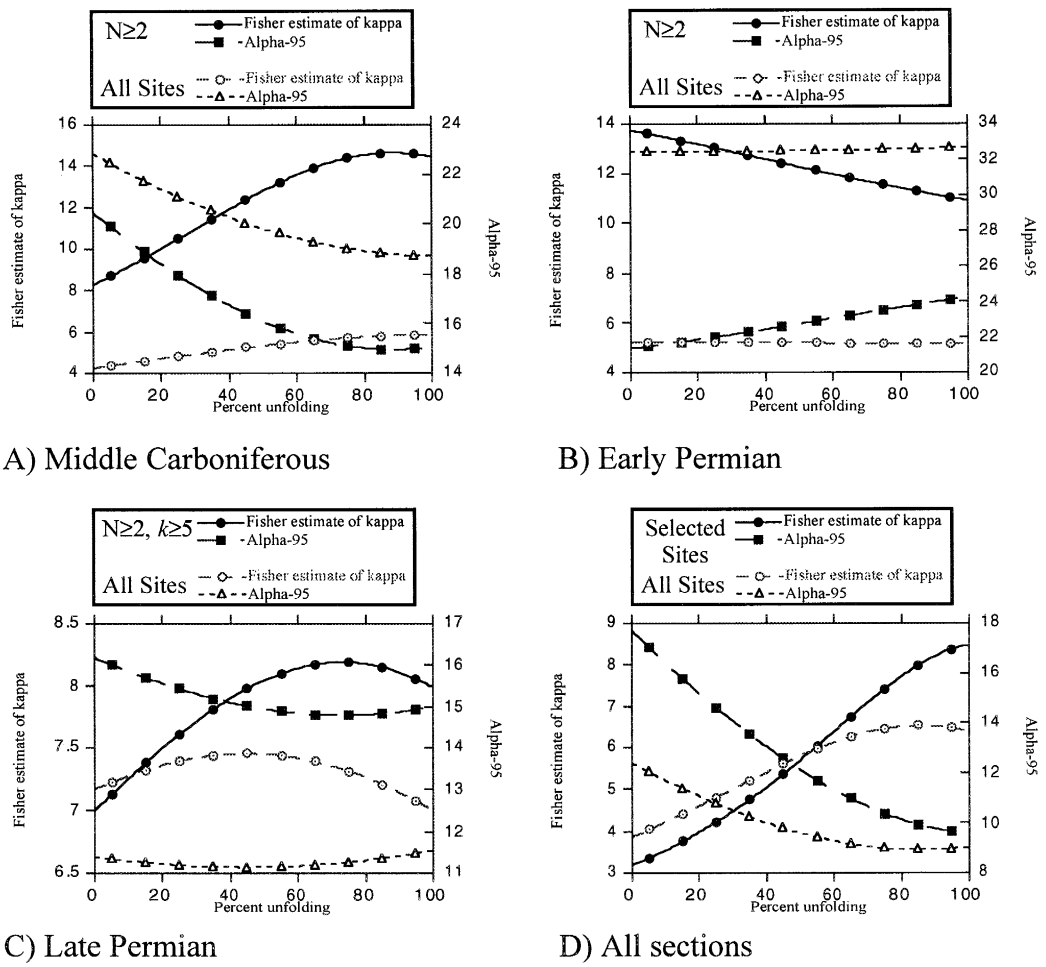

Fig. 7. Summary of B component paleomagnetic data unfolding statistics for (A) Bashkirian and Moscovian epochs of the Late Carboniferous (Middle Carboniferous using the U.S.S.R. system) sites, (B) Early Permian sites, (C) Late Permian sites and (D) all sites. For the Bashkirian and Moscovian epochs of the Late Carboniferous (Middle Carboniferous) and Early Permian statistics for sites with N (samples) ≥ 2 only and all sites are plotted. For the Late Permian aged samples statistics calculated using all sites and only sites with N (samples) ≥ 2 and k-value ≥ 5 are plotted. In D, the selected sites consist of N (samples) ≥ 2 (Middle Carboniferous and Early Permian) and N (samples) ≥ 2 and k-value ≥ 5 (late Permian) sites. Numeric data are given in Table 1.

was observed in the Late Permian section near Bilik-tui village. The units were sampled in two, non-overlapping, stratigraphic sections, corresponding to the east (7 sites) and west (19 sites) margins of the Bereya river valley. Site mean directions show similar grouping in both geographic and stratigraphic coordinates, however the site mean directions are of two magnetic polarities. Sites were unfolded at 1% increments in an incremental fold test. We calculated the statistics for all sites with $n \geq 2$ ($N = 25$) and using sites for which $n \geq 2$ and k-value ≥ 5 ($N = 14$). Using all sites with $n \geq 2$, there was no significant change in the k-value during unfolding for the tilt of the sampled units (k_{100}-value/k_0-value = 1.01, $n = 25$; Fig. 7), because of a coincidence of the direction of remanent magnetizations and the strike of bedding corrections. For sites with $n \geq 2$ and k-value ≥ 5, the k-value changes from $k_0 = 7.00$, to k_{73}-value = 8.19, to k_{100}-value = 7.99. The mean direction is not similar with the A component, PDF, or present-day dipole magnetic field directions ($I_g = 19.2°$, $D_g = 69.3°$, k-value = 7.00, $\alpha_{95} = 16.2°$, $n = 14$; Fig. 8). The paleolatitude and A-95 calculated from the Fisher average of site paleomagnetic poles is $19.6° \pm 14.5°$.

Table 3
Statistical analysis of the B component

Age	N	I_g	D_g	k-value	α_{95}	I_s	D_s	k-value	α_{95}
C^*_{2A}	13	28.2	100.1	4.3	22.8	33.8	82.3	5.9	18.7
C^*_{2B}	8	21.0	113.8	8.3	20.5	34.4	98.8	14.5	15.1
P_1	6	58.7	210.5	5.2	32.5	46.5	82.2	5.2	32.7
P^*_1	5	59.8	232.2	13.8	21.4	50.4	66.8	10.9	24.3
Tr	3	37.8	88.8	4.36	68.0	35.0	65.3	4.37	68.0
P_2	26	27.0	78.1	7.17	11.4	36.0	103.6	7.00	11.6
P^*_2	14	19.2	69.3	7.00	16.2	37.3	87.9	7.99	15.0

C^*_{2A}, C^*_{2B}, Bashkirian and Moscovian epochs of the late Carboniferous; P_1, P^*_1, Early Permian; P_2, P^*_2, Late Permian and Tr, Triassic. C^*_{2A}, P_1, Tr and P_2 mean directions were calculated using all sites. C^*_{2B} and P^*_1 mean directions were calculated using sites with n (samples) ≥ 2. The P^*_2 mean direction was calculated using late Permian sites with $n \geq 2$ and k-value ≥ 5. The optimum grouping of C^*_{2B} ($n = 8$) was at 88% unfolding, $I_{88\%} = 33.2°$, $D_{88\%} = 101.2°$, k-value = 14.6 and $\alpha_{95} = 15.0°$. The optimum grouping of P^*_2 ($n = 14$) was at 73% unfolding, $I_{73\%} = 33.7°$, $D_{73\%} = 81.3°$, k-value = 8.2 and $\alpha_{95} = 14.8°$. Stratigraphic coordinate paleomagnetic poles calculated from Fisher averaging site virtual geomagnetic poles are, C^*_{2B}, $\lambda_s = 10.2°$, $\phi_s = 186.2°$, k-value = 15.0, $A_{95} = 14.8°$, $N = 8$; P^*_1, $\lambda_s = 33.8°$, $\phi_s = 207.8°$, k-value = 9.4, $A_{95} = 26.3°$, $N = 5$; P^*_2, $\lambda_{73\%} = 20.5°$, $\phi_{73\%} = 200.6°$, k-value = 8.5, $A_{95} = 14.5°$, $N = 14$.

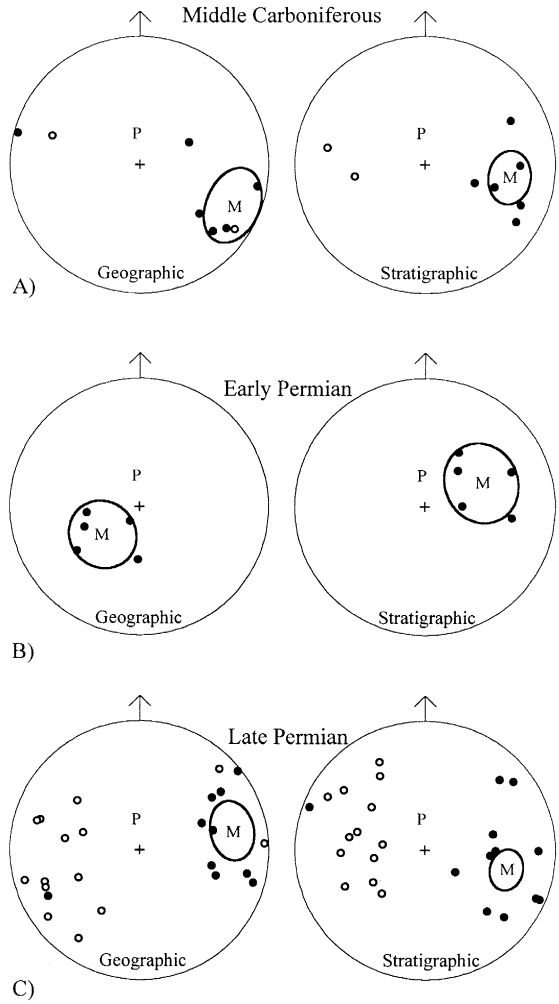

Fig. 8. Summary of B component paleomagnetic site mean directions from the (A) Bashkirian and Moscovian epochs of the late Carboniferous (Middle Carboniferous using the U.S.S.R. system), (B) Early Permian and (C) Late Permian sections. The location of the mean site directions, the overall Fisher mean M, α_{95} cone of confidence and the present-day magnetic field direction P are shown in geographic and stratigraphic coordinates. Solid symbols are lower hemisphere directions, open symbols are upper hemisphere directions. Numerical data are given in Tables 1 and 3.

5. Interpretation of the A component

The lower unblocking temperature component, component A, fails the fold test, is always of down-

ward directed magnetic inclination, and may record the present-day earth's (PDF) magnetic field [PDF $I = 69.4°$, $D = 351.8°$; component A, $I_g = 65.1°$, $D_g = 356.5°$, $\alpha_{95} = 6.2°$, N (sites) = 50].

The A magnetization may represent a post-folding overprint of Cretaceous age. Descriptions of the regional geology suggest that Early Cretaceous plutonism occurred along this portion of the southern Siberian plate margin. The expected inclination of an overprinting Early or Late Cretaceous direction, calculated using the European references poles of Van der Voo (1993) closely match the PDF inclination in this region and the observed A component inclination. If the A component represents an Early Cretaceous aged overprint, comparing the expected and observed declinations suggests that post-overprinting counter-clockwise rotation of these sampled units may have occurred.

6. Interpretation of the B component

The overall interpretation of these B components is problematical. We cannot constrain the age of folding of the sampled units. In the Late Permian section there is a relatively larger number of sites, 26

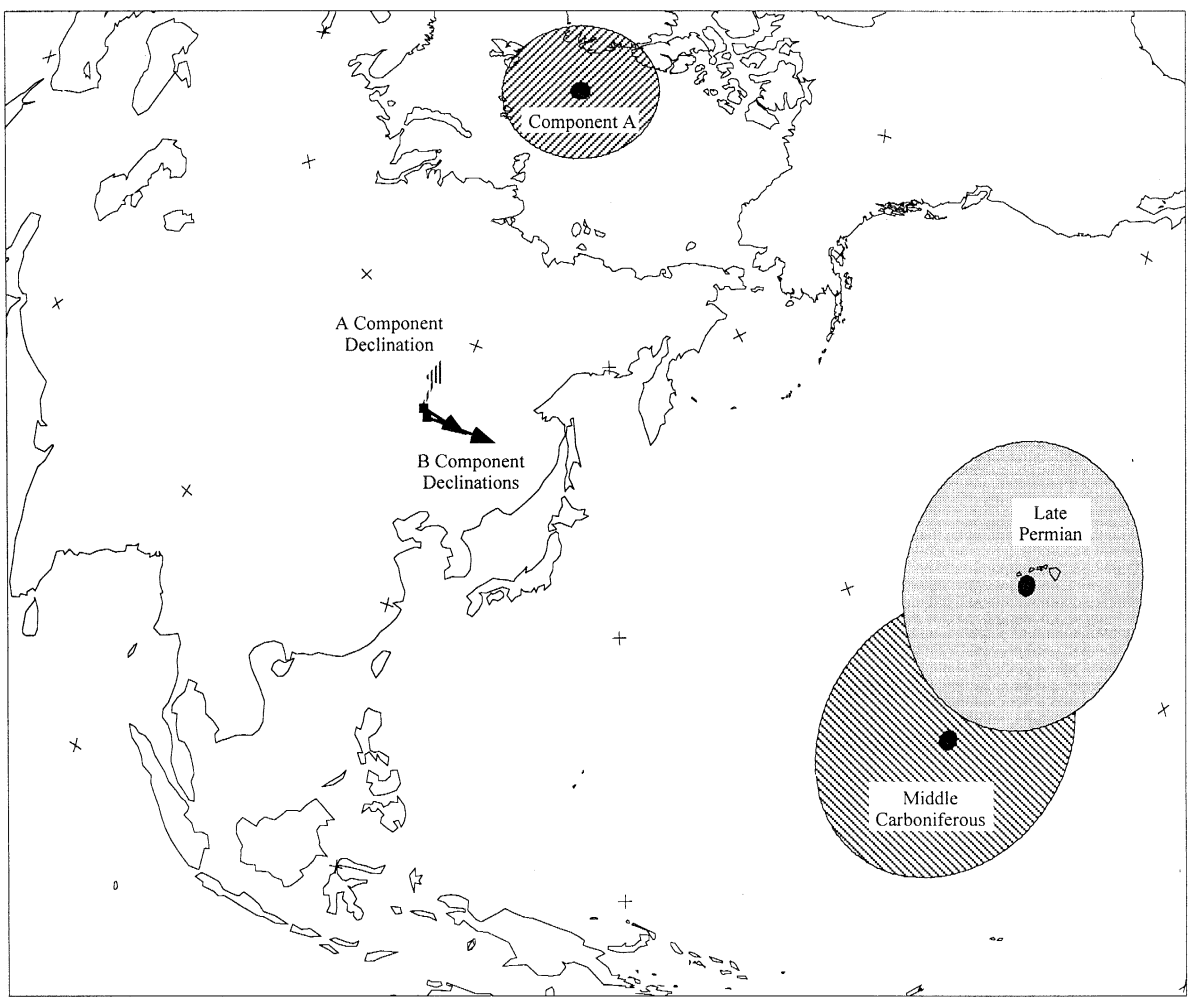

Fig. 9. Summary of paleomagnetic poles calculated in this study from the A and B components. Geographic coordinate declination for the A component (non-solid arrow) and optimum or stratigraphic coordinate declination for the B components (solid arrows) are also shown.

overall and 14 sites with n (samples) ≥ 2 and k-value ≥ 5, which appear to record two polarities of magnetization. The Bashkirian to Moscovian epochs age sites also record two magnetic polarities and appear to have better grouping in stratigraphic coordinates. The paleomagnetic pole calculated from the stratigraphic mean of either B_{MC} or the B_{LP} direction is not similar to that calculated from the A component, PDF pole, or the present-day dipole location (Fig. 9). On the basis of these observations we interpret the B_{MC} and B_{LP} components to represent a characteristic remanent magnetization ac-

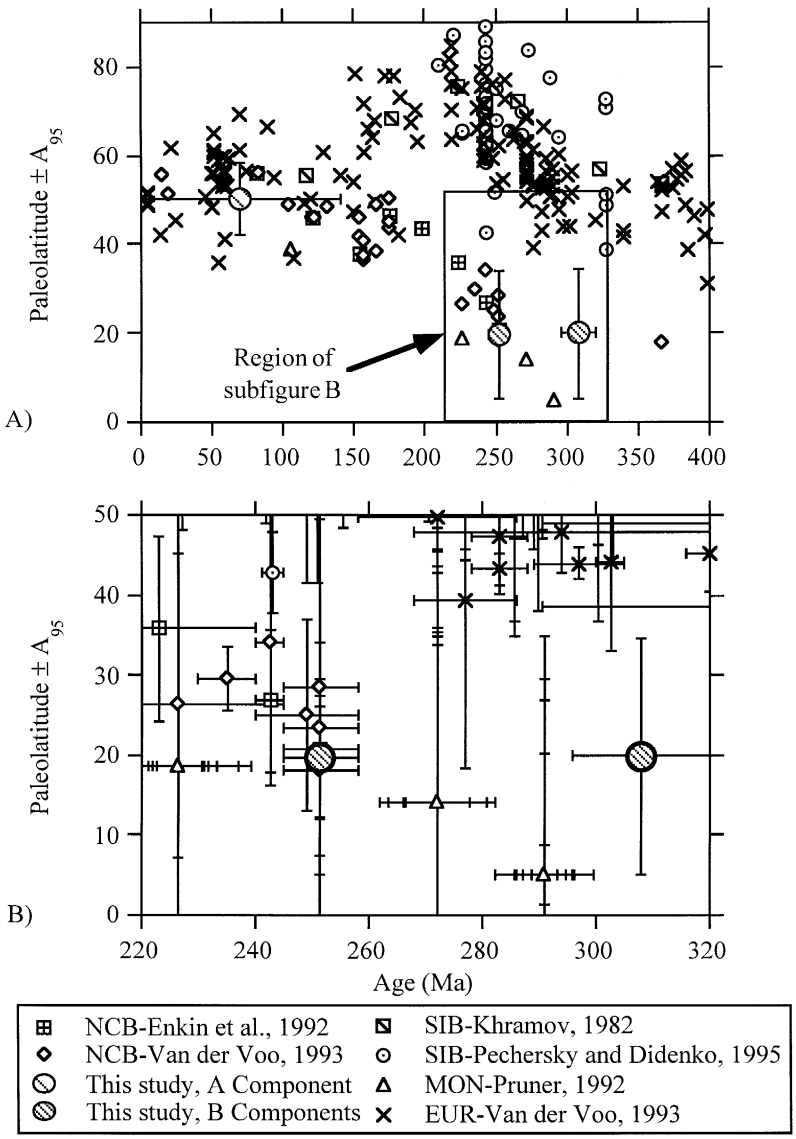

Fig. 10. Comparison of the expected paleolatitudes for Bashkirian and Moscovian epochs of the Late Carboniferous, Early Permian and Late Permian calculated from the paleomagnetic poles shown in Fig. 7Fig. 8Fig. 9, with the expected paleolatitudes calculated from references poles for Siberia (SIB, Khramov, 1982; Pechersky and Didenko, 1995), Europe (EUR, Van der Voo, 1993), Mongolia (MON, Pruner, 1992) and North China Block (NCB, Enkin et al., 1992 and Van der Voo, 1993). (A) Comparison between 100 and 500 Ma. (B) Comparison between 225 and 325 Ma showing uncertainties in ages and paleolatitudes.

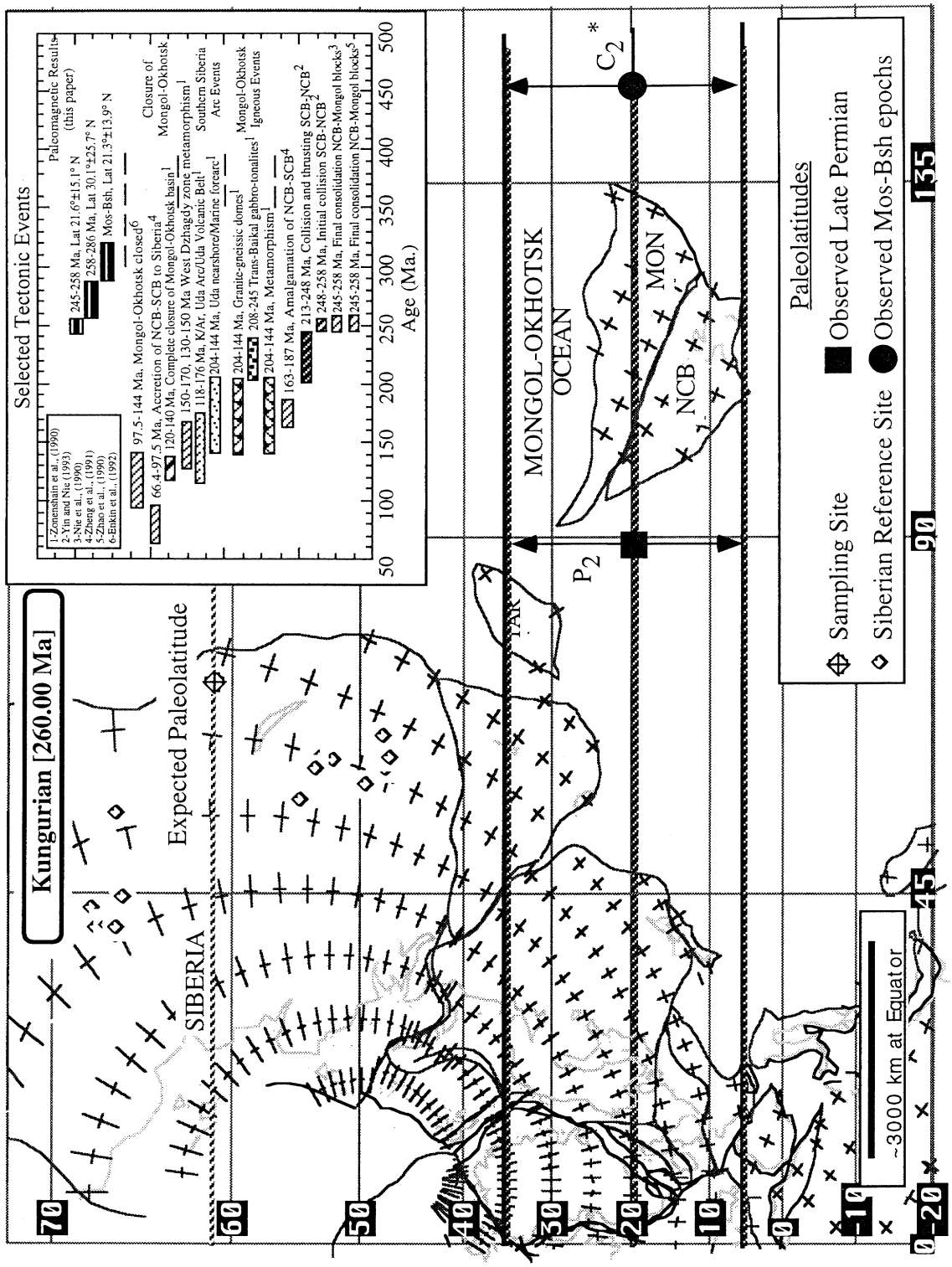

Fig. 11. Paleogeographic reconstruction of eastern Asia tectonic elements at 260 Ma. The paleolatitudes (including A_{95} uncertainties) observed in the Bashkirian and Moscovian epochs of the Late Carboniferous and Late Permian aged sections closely match those expected from reference studies of similar ages from the Mongolian composite terranes (*MON*) or North China Block (*NCB*). The paleogeographic locations of the Tarim (*TAR*), MON and NCB terranes are taken from Enkin et al. (1992).

quired during or shortly after deposition of these respective units during the Bashkirian to Moscovian epochs or Late Permian. The paleolatitude calculated from these paleomagnetic poles can be compared with the reference paleomagnetic data from the Siberian and Eurasia plates, and North China block.

There are alternative interpretations for the B component. Given our relatively poor understanding of the precise geology, fault structures, and age of folding in these sampling regions an acceptable alternative model of the B component is that of a two-polarity remagnetization. An overall fold test of selected sites which show a B component, using sites with n (samples) ≥ 2, for the Bashkirian to Moscovian epochs of the Late Carboniferous and Triassic and Early Permian and sites with n (samples) ≥ 2 and k-value ≥ 5 for the Late Permian, shows an initially poor grouping ($k\text{-value}_{0\%} = 3.2$) in geographic coordinates which improves with incremental unfolding [$k\text{-value}_{100\%} = 8.5$, n (sites) $= 30$]. The overall mean inclination is initially shallow ($I_g = 35.7°$) and remains so during incremental unfolding ($I_s = 39.1°$). Using the reference paleomagnetic poles for the European (Van der Voo, 1993) or Siberian cratons (Khramov, 1982; Pechersky and Didenko, 1995) no such shallow inclinations are expected for this region for any younger time in which remagnetization of the sampled units may have occurred adjacent to Siberia.

For comparison with the stable European plate, we used the reference paleomagnetic data compiled in Van der Voo (1993). The expected paleolatitude for a representative location in our sampling region ($\lambda = 51°$N, $\phi = 116°$E) is between 60°N–70°N during the Triassic and Permian. Paleomagnetic reference data for the Siberian plate from Khramov (1982) and Pechersky and Didenko (1995) yield expected northerly paleolatitudes of between 65°N and 80°N. These expected paleolatitudes are significantly different from the paleolatitude of Bashkirian to Moscovian section of $\lambda_{MC} = 19.9° \pm 14.8°$ or the $\lambda_{P2} = 19.6° \pm 14.5°$ observed in the Late Permian section which we sampled. The means of the Triassic and Early Permian sites, which recorded only a single magnetic polarity, are also of a lower paleolatitude when compared with these Siberian or European reference studies (Fig. 10).

An alternative remagnetization model is that the B component represents a secondary component acquired while the units were located near the MON-NCB composite terrane. Possible ages of overprinting may be constrained by the mean of the three Triassic sites. The mean direction of these sites changes from $D_g = 88.8°$ $I_g = 37.8°$ to $D_s = 65.3°$ $I_s = 35.0°$, n (sites) $= 3$, similar with the other B component directions. There are Triassic–Jurassic age igneous events described by Zonenshain et al. (1990) including metamorphism and formation of granite–gneissic domes which may suggest a post-Triassic two polarity overprint origin of the B component. In this model, the overall inclination for all sites suggests significant poleward movement of the paleomagnetically sampled units after overprinting occurred.

Using reference paleomagnetic poles from the North China block to calculate paleolatitudes for this site, yields expected paleolatitudes of between 10°N to 30°N (Van der Voo, 1993; Enkin et al., 1992) during Permian and Triassic. These expected paleolatitudes are compatible with the reconnaissance results from this paleomagnetic study. Our interpretation of the Carboniferous and Late Permian paleolatitudes calculated from the B component are that the sampled stratigraphic sections within the Mongol–Okhotsk belt may have been located at a low paleolatitudes during their deposition (Fig. 11). The interpretation of low paleolatitudes for this region of the Mongol–Okhotsk belt is in agreement with the model proposed by Enkin et al. (1992). A complicating factor is that the observed declinations are rotated significantly clockwise. Whether this rotation is related to local rotation or rotation during poleward motion is not clear.

7. Conclusions

In this study of the paleomagnetism of Bashkirian to Moscovian epochs of the Late Carboniferous, Early Permian, Late Permian and Triassic units from the Chita region of southern Russia, two magnetic components are observed. The A component was observed in all sections, is of downward directed magnetic inclination and fails the fold test.

A higher unblocking temperature, B component is observed in the Bashkirian to Moscovian epochs of

the Late Carboniferous, Early Permian, Late Permian and Triassic sections. Only three sites were collected from the Triassic units and no meaningful error parameters can be calculated. The Bashkirian to Moscovian epochs age section, using sites with $n \geq 2$, gives site mean directions which are best grouped in stratigraphic coordinates and record two magnetic polarities. The corresponding Bashkirian to Moscovian epochs of the Late Carboniferous paleolatitude is $\lambda = 19.9° \pm 14.8°$. The Late Permian paleolatitude is $\lambda = 19.6° \pm 14.5°$, calculated from sites of two polarities which show slightly better grouping in stratigraphic coordinates. The age of magnetization of the Early and Late Permian aged units is uncertain because there is no significant change in the Fisher estimate of kappa during incremental unfolding of these sites, and thus no fold test. These directions are not similar to an expected overprinting magnetic field direction and in the Bashkirian to Moscovian epochs of the Late Carboniferous and Late Permian sections are recorded by sites of downward and upward directed magnetic inclination. An interpretation of these magnetizations is that they may represent the characteristic remanent magnetization acquired shortly after or during deposition of these units, although this interpretation is highly uncertain. The corresponding paleolatitudes suggest that significant displacement with respect to the European or Siberian plates has occurred since the Paleozoic. The paleolatitudes of these units are similar to that expected from reference paleomagnetic poles of the corresponding ages from the North China block. These data may be interpreted to suggest that Paleozoic aged rock units of the Chita region, presently located in southern Russia, may have been closely associated with the Mongolia and North China blocks during their deposition.

Acknowledgements

We wish to dedicate this study to the memory of the late Dr. Lev Zonenshain. Dr. Zonenshain was an enthusiastic, youthful and energetic colleague and friend. The recent volume dedicated in his memory (Han and Mossakovskee, 1995) is a wonderful reminder of his personality and contributions. This project was made possible by a National Academy of Sciences–Academy of the U.S.S.R. scientific exchange program grant to Harbert and our field program. We thank Dr. M. Kuzmin for his strong support of this project. The work of Mark Kazimirovskiy and Valeriy Michailov in the field is gratefully acknowledged. We also thank the editor and staff of *Tectonophysics* and Drs. Randy Enkin and Rob Van der Voo for their help on this manuscript. These reviews and the important corrections and clarifications they contained added to the manuscript and greatly improved it.

References

Enkin, R., Yang, Z., Chen, Y. and Courtillot, V., 1992. Paleomagnetic constraints on the geodynamic history of the major blocks of China from the Permian to the Present. J. Geophys. Res., 97: 13,953–13,989.

Han, V.E. and Mossakovskee, A.A., 1995. Lev Pavlovich Zonenshain, A Collection of Reminiscences (in Russian). Nauka, Moscow, 328 pp.

Harland, W., Cox, A., Llewellyn, P., Pickton, C., Smith, A. and Walters, R., 1982. A Geologic Time Scale. Cambridge University Press, 131 pp.

Khramov, A. N., 1982. Paleomagnetology (in Russian). Nedra, Leningrad, 312 pp.

Li, Y., 1990. An apparent polar wander path from the Tarim block, China. Tectonophysics, 181: 31–41.

Li, Y., McWilliams, M.O., Cox, A., Sharps, R., Li, Y.A., Gao, Z., Zhang, Z. and Zhai, Y., 1988a. Late Permian paleomagnetic pole from dikes of the Tarim craton, China. Geology, 16: 275–278.

Li, Y., Zhang, Z., McWilliams, M.O., Sharps, R., Zhai, Y., Li, Y.A., Li, Q. and Cox, A., 1988b. Mesozoic paleomagnetic results of the Tarim craton Tertiary relative motion between China and Siberia. Geophys. Res. Lett., 15: 217–220.

Li, Y., McWilliams, M.O., Sharps, R., Cox, A., Li, Y., Li, Q., Gao, Z., Zhang, Z. and Zhai, Y., 1990. A Devonian paleomagnetic pole from red beds of the Tarim Block, China. J. Geophys. Res., 95: 19,185–19,198.

Li, Y., Sharps, R., McWilliams, M., Li, Y., Li, Q. and Zhang, W., 1991. Late Paleozoic paleomagnetic poles from the Jungar Block, northwestern China. J. Geophys Res., 96: 16,047–16,060.

Li, Y., Sharps, R., McWilliams, M.O., Nur, A., Li, Y. A., Li, Q. and Zhang, W., 1989. Paleomagnetic results from dikes of the Jungar block, northwestern China. Earth Planet. Sci. Lett., 94: 123–130.

Li, Y. and Zhang, Z., 1986. Preliminary Paleomagnetic Results of the Late Paleozoic from the Qiliangshan Terrane. J. Changchun Geol. Inst., 46(4).

Lin, J.L. and Fuller, M.D., 1986. Mesozoic and Cenozoic evolution of the North and South China Blocks. Nature, 320: 87.

Lin, J.L., Fuller, M. and Zhang, W., 1985. Preliminary Phanerozoic polar wander paths for the North and South China Blocks. Nature, 313: 444–449.

McElhinny, M.W. and Lock, J., 1990. Global Paleomagnetic Database Project. Phys. Earth Planet. Inter., 63: 1–6.

McFadden, P.L., Ma, X., McElhinny, M.W. and Zhang, Z., 1988. Permo-Triassic magnetostratigraphy in China: northern Tarim. Earth Planet. Sci. Lett., 87: 152–160.

Nie, S., 1991. Paleoclimatic and paleomagnetic constraints on the Paleozoic reconstructions of South China, North China and Tarim. Tectonophysics, 196: 279–308.

Nie, S., Rowley, D.B. and Ziegler, A.M., 1990. Constraints on the location of the Asian microcontinents in Paleo-Tethys during the late Paleozoic. In: W.S. McKerrow and C.R. Scotese (Editors), Paleozoic Paleogeography and Biogeography. Geol. Soc. London Mem., 12: 397–409.

Nie, S., Rowley, D., Van der Voo, R. and Maosong, L., 1993. Paleomagnetism of late Paleozoic rocks in the Tianshan, northwestern China. Tectonics, 12: 568–579.

Pechersky, D.M. and Didenko, A.N., 1995. Paleozoic Ocean, Petromagnetic and Paleomagnetic Information of the Lithosphere (in Russian). OEFZ RAN Publishers, Moscow, 296 pp.

Pruner, P., 1987. Paleomagnetism and Paleogeography of Mongolia in the Cretaceous, Permian and Carboniferous — preliminary data. Tectonophysics, 139: 155–167.

Pruner, P., 1992. Paleomagnetism and Paleogeography of Mongolia in the Cretaceous, Permian and Carboniferous — final report. Phys. Earth Planet. Inter., 70: 169–177.

Sharps, R., McWilliams, M.O., Li, Y., Cox, A., Zhang, Z., Zhai, Y., Gao, Z., Li, Y.A. and Li, Q., 1989. Lower Permian paleomagnetism of the Tarim block, northwestern China. Earth Planet. Sci. Lett., 92: 275–291.

Van der Voo, R., 1993. Paleomagnetism of the Atlantic, Tethys and Iapetus Oceans. Cambridge University Press, 411 pp.

Yin, A. and Nie, S., 1993. An indentation model for the north and south China collision and the development of the Tan-Lu and Honam fault systems, eastern Asia, Tectonics, 12: 801–813.

Zhao, X. and Coe, R.S., 1987. Paleomagnetic constraints on the collision and rotation of North and South China. Nature, 327: 141–144.

Zhao, X., Coe, R S., Zhou, Y., Wu, H. and Wang, J., 1990. New paleomagnetic results from northern China: collision and suturing with Siberia and Kazakhstan. Tectonophysics, 181: 43–81.

Zheng, Z., Kono, M., Tsunakawa, H., Kimura, G., Wei, Q., Zhu, X. and Hao, T., 1991. The apparent polar wander path for the North China Block since the Jurassic. Geophys. J. Int., 104: 29–40.

Zonenshain, L.P., Kuzmin, M.I. and Natapov, L.M., 1990. Geology of the USSR: A Plate-Tectonic Synthesis. In: B.M. Page (Editor), Geodynamics Series, vol. 21. Am. Geophys. Union, 242 pp.